Structure of Ni^{2+} Solutions in Ethylene Glycol by Neutron Diffraction: An Observed Hydrogen Bond between the Solvent Ligands in the First and Second Cation Coordination Shells?

Paul B. Lond, Philip S. Salmon,* and David C. Champeney

Contribution from the School of Physics, University of East Anglia, Norwich NR4 7TJ, U.K.
Received March 4, 1991

Abstract: The method of isotopic substitution in neutron diffraction is applied to study the coordination environment of the Ni^{2+} ion in a 0.956 *m* solution of $Ni(CF_3SO_3)_2$ in fully deuterated ethylene glycol (EG). It is shown that EG molecules do not act as monodentate ligands but that $Ni(EG)_3^{2+}$ tris-chelate complexes are formed. There is no evidence of inner-sphere complexing by the $CF_3SO_3^-$ anion, but the data are consistent with a spatially well defined hydrogen bond between EG ligands in the first and second coordination shells of the cation. If this bond is assumed to be linear, then it is of length $\sim$1.8 (1) Å. The number of second-shell EG molecules that participate in this hydrogen-bond process is estimated at six. Furthermore, there is evidence for weak ordering of the Ni^{2+} correlations on a length scale of $10 \lesssim r$ (Å) $\lesssim 16$. The stability of the $Ni(EG)_3^{2+}$ complex is briefly discussed.

Introduction

There is considerable interest in the coordination chemistry of ions in solvent media owing to its importance in the understanding of kinetic processes such as solvent exchange, transport properties such as ionic mobility, and other electrochemical effects. While over the years many results on the structure of electrolyte solutions have been obtained, there is still very little experimental information at the pair-distribution function level, except in the case of aqueous ionic solutions.[1,2] Much of the most detailed information at this level has been provided by the isotopic substitution method in neutron diffraction.[1] This follows since all correlations, except those involving the isotopically substituted species, can be eliminated from the total diffraction pattern and information on the structure beyond the immediate nearest neighbors is obtained. In view of previous work on the Ni^{2+} ion in aqueous and methanolic solution and the general dearth of knowledge on nonaqueous ionic solutions at the pair-distribution function level, we have applied the isotopic substitution method to study the coordination environment of Ni^{2+} in a 0.956 *m* (mol kg^{-1}) solution of $Ni(CF_3SO_3)_2$ in fully deuterated ethylene glycol (ethane-1,2-diol). The trifluoromethanesulfonate (or triflate) anion was chosen as the counterion since it has a tendency to be weakly nucleophilic in solution,[3] it is possible to safely prepare dry triflate salts,[4] and $Ni(CF_3SO_3)_2$ salts have a relatively high solubility in nonaqueous media.[5]

Part of the interest in the higher alcohols ethylene glycol (EG) and glycerol stems from certain similarities between these alcohols and water. For example, all three liquids are hydrogen bonded,[6-8] and they have large relative permittivities, which makes them good solvents for ionic salts. It is also of interest that the partial molal volumes of alkali-metal halides dissolved in EG[9] are quite close to those in water. Furthermore the ratio of the ionic mobilities of alkali-metal and halide ions are approximately the same in all three solvents,[10] although the absolute values do of course scale approximately with the solvent viscosity. In contrast, measurements of the ionic mobilities in solutions of $NiCl_2$ have shown that the nickel transference number decreases markedly in the solvent order water, EG, glycerol.[11] It is natural to wonder whether this behavior in the divalent cations is due to large long-lived ion-solvent complexes.

Further motivation for the present study has been provided by recent attempts at modeling the structure of the higher alcohols using molecular dynamics methods.[12] Detailed experimental information on the structure of the higher alcohol systems at the pair-distribution function level is important if the computations are to be developed and extended to ionic solutions.

In the first part of this paper, the essential theory behind the isotopic substitution method in neutron diffraction, as applied to ionic solutions, is outlined. Next the experimental method and results are given. The results are discussed in terms of the nature of the Ni^{2+}-EG molecule complex, previous results on Ni^{2+} complexes in solution, and the possibility that they can be fully explained in terms of a well-defined hydrogen bond between the first and second solvation shell EG ligands.

Theory

The isotopic substitution method in neutron diffraction, as applied to the problem of ionic solutions, has been described in detail elsewhere.[1] To summarize, diffraction experiments are conducted on two fully deuterated solutions in ethylene glycol that are identical in every respect except for the isotopic composition of the Ni^{2+} ion. Deuterated solvents are preferred owing to the large incoherent cross-section of hydrogenated materials. Each measured intensity is then corrected for background, placed on an absolute scale by comparison with the diffraction pattern from a vanadium standard, and corrected for multiple and container scattering as well as for the attenuation of the beam by the sample and container materials.[13] The quantity thus derived is, for each solution, a total structure factor $F_0(k)$ given by

$$F_0(k) = F(k) + \sum_{\alpha=1}^{\mu} c_\alpha \frac{\sigma_\alpha^s}{4\pi} + \epsilon(k) \qquad (1)$$

where k is the scattering vector, c_α and σ_α^s are, respectively, the atomic fraction and total bound (coherent and incoherent) scattering cross-section of species α, and μ (=6) is the total number

* To whom correspondence should be addressed.

(1) Enderby, J. E.; Cummings, S.; Herdman, G. J.; Neilson, G. W.; Salmon, P. S.; Skipper, N. *J. Phys. Chem.* **1987**, *91*, 5851.
(2) Magini, M.; Licheri, G.; Pashina, G.; Piccaluga, G.; Pinna, G. *X-ray Diffraction of Ions in Aqueous Solutions: Hydration and Complex Formation*; CRC Press: Boca Raton, FL, 1988.
(3) Taube, H.; Scott, A. *Inorg. Chem.* **1971**, *10*, 62.
(4) Jansky, M. T.; Yoke, J. T. *J. Inorg. Nucl. Chem.* **1979**, *41*, 1707. Howells, R. D.; McCown, J. D. *Chem. Rev.* **1977**, *77*, 69.
(5) Takei, T. *Surf. Technol.* **1984**, *23*, 73. *Surf. Coat. Technol.* **1987**, *31*, 163.
(6) Neilson, G. W.; Enderby, J. E., Eds. *Water and Aqueous Solutions*; Adam Hilger: Bristol, 1986.
(7) Podo, F.; Némethy, G.; Indovina, P. L.; Radics, L.; Viti, V. *Mol. Phys.* **1974**, *27*, 521.
(8) Champeney, D. C.; Joarder, R. N.; Dore, J. C. *Mol. Phys.* **1986**, *58*, 337. Garawi, M.; Dore, J. C.; Champeney, D. C. *Mol. Phys.* **1987**, *62*, 475.
(9) Zana, R.; Yeager, E. B. In *Modern Aspects of Electrochemistry No 14*; Bockris, J. O.'M., Conway, B. E., White, R. E., Eds.; Plenum Press: New York, 1982; Chapter 1, p 42.
(10) Santos, M. C.; Spiro, M. *J. Phys. Chem.* **1972**, *76*, 712. Blanco, M. C.; Champeney, D. C.; Kameche, M. *Phys. Chem. Liq.* **1989**, *19*, 163.
(11) Blanco, M. C.; Champeney, D. C. *Phys. Chem. Liq.* **1991**, *23*, 93.
(12) Root, L. J.; Stillinger, F. H. *J. Chem. Phys.* **1989**, *90*, 1200.
(13) Salmon, P. S. *J. Phys. F: Met. Phys.* **1988**, *18*, 2345.

0002-7863/91/1513-6420$02.50/0

Table I. Experimental Details of the Solutions

solute	m (mol kg^{-1})	designation of scattering pattern	density at 23 °C (g cm^{-3})	n_0 (atom $Å^{-3}$)	total scattering cross-section (b)[a]	total absorption cross-section at 0.7042 Å (b)[b]
$^{N}Ni(CF_3SO_3)_2$	0.953 (2)	$^{N}F_0(k)$	1.400 (2)	0.1027	3.896 (6)	0.0140 (4)
$^{62}Ni(CF_3SO_3)_2$	0.958 (2)	$^{62}F_0(k)$	1.402 (2)	0.1025	3.846 (6)	0.0364 (8)

[a] Calculated by using the free atom cross-sections.[17] [b] Reference 17.

of chemical species in the solution. The most prominant contribution to the correction term $\epsilon(k)$ arises because of a departure from the static approximation in the case of neutron scattering from liquids and is a particular problem when light nuclei are present.[14] $F(k)$ is a linear sum of the partial structure factors, $S_{\alpha\beta}(k)$, whose Fourier transforms (FT) yield the partial pair-distribution functions $g_{\alpha\beta}(r)$:

$$F(k) = \sum_{\alpha}\sum_{\beta} c_\alpha c_\beta b_\alpha b_\beta [S_{\alpha\beta}(k) - 1] \quad (2)$$

with

$$g_{\alpha\beta}(r) = 1 + \frac{1}{2\pi^2 n_0 r}\int_0^\infty [S_{\alpha\beta}(k) - 1] k \sin(kr)\, dk \quad (3)$$

where b_α is the coherent scattering length of species α and n_0 is the total atomic number density of the solution. $g_{\alpha\beta}(r)$ gives a measure of the probability of finding an atom of species β at a distance r from an atom of type α located at the origin of coordinates. It is defined so that the mean number of particles of type β contained in the volume defined by two concentric spheres of radii r_1 and r_2, centered on a particle of type α, is given by

$$\bar{n}_\beta^\alpha = 4\pi n_0 c_\beta \int_{r_1}^{r_2} r^2 g_{\alpha\beta}(r)\, dr \quad (4)$$

Equation 4 was used to determine coordination numbers in the present work.

In the solution studied here, $F(k)$ comprises 21 $S_{\alpha\beta}(k)$ functions. However, if the coherent scattering length of the cation is changed by substituting enriched nickel isotope (^{62}Ni, b_{Ni}) in place of nickel having the natural isotopic abundance (^{N}Ni, b_{Ni}), subtraction of the two corresponding $F_0(k)$ functions (eq 1) gives

$$\Delta_{Ni}{}^0(k) \equiv {}^{N}F_0(k) - {}^{62}F_0(k) = \Delta_{Ni}(k) + \frac{c_{Ni}}{4\pi}\{\sigma_{Ni}{}^s - \sigma_{'Ni}{}^s\} + \epsilon'(k) \quad (5)$$

where

$$\Delta_{Ni}(k) = A[S_{NiO}(k) - 1] + B[S_{NiD}(k) - 1] + C[S_{NiC}(k) - 1] + D[S_{NiS}(k) - 1] + E[S_{NiF}(k) - 1] + F[S_{NiNi}(k) - 1]$$

with

$$\Delta b = b_{Ni} - b_{'Ni}$$

$$A = 2c_{Ni}c_O b_O \Delta b \qquad B = 2c_{Ni}c_D b_D \Delta b$$

$$C = 2c_{Ni}c_C b_C \Delta b \qquad D = 2c_{Ni}c_S b_S \Delta b$$

$$E = 2c_{Ni}c_F b_F \Delta b \qquad F = c_{Ni}{}^2\{b_{Ni}{}^2 - b_{'Ni}{}^2\} \quad (6)$$

An important property of the difference function $\Delta_{Ni}{}^0(k)$ is that the $\epsilon(k)$ terms in $F_0(k)$ are, to first order, eliminated so that the remaining correction terms $\epsilon'(k)$ are then sufficiently small to be neglected.[1] The real-space picture is obtained from

$$\Delta G_{Ni}(r) = \frac{1}{2\pi^2 n_0 r}\int_0^\infty \Delta_{Ni}(k) k \sin(kr)\, dk = A[g_{NiO}(r) - 1] + B[g_{NiD}(r) - 1] + C[g_{NiC}(r) - 1] + D[g_{NiS}(r) - 1] + E[g_{NiF}(r) - 1] + F[g_{NiNi}(r) - 1] \quad (7)$$

The efficacy of the correction procedures can be tested on two accounts. Firstly, since $S_{\alpha\beta}(k) \to 1$ in the limit as $k \to \infty$, $\Delta_{Ni}{}^0(k)$ should oscillate about the calculated $c_{Ni}\{\sigma_{Ni}{}^s - \sigma_{'Ni}{}^s\}/4\pi$ value provided $\epsilon'(k)$ is negligible.[15] Secondly, since $g_{Ni\beta}(r) = 0$ at r values below the distance of closet approach to the Ni^{2+} ion, $\Delta G_{Ni}(r)$ should be equal to the calculated $\Delta G_{Ni}(0) = -(A + B + C + D + E + F)$ at low r.

Experimental Method

Natural nickel powder (Aldrich, Gold Label) or ^{62}Ni (1.52% ^{58}Ni, 1.13% ^{60}Ni, 0.12% ^{61}Ni, 97.01% ^{62}Ni, 0.22% ^{64}Ni, Oak Ridge, USA) powder was dissolved in HCl (Fisons, 99.999%). The nickel was then precipitated as the hydroxide by addition of NaOH (BDH, Analar), and the precipitate was rinsed with deionized water in a Buchner funnel. A solution of 25% HCF_3SO_3 (Sigma, 98%) in water was used to give nickel triflate, which was then baked on a hot plate to remove any excess acid. Next the salt was redissolved, filtered, baked again, ground to a fine powder, and dried under vacuum at ~160 °C for ~37 h to form an anhydrous yellow solid.[4]

The solutions were made by weight in a high-purity argon-filled glovebox by using fully deuterated EG (99% enrichment, Cambridge Isotope Laboratories, USA). The concentrations were checked by first passing an aliquot of the electrolyte through an ion exchange column (BDH, Amberlite IR120H resin). The eluted acid was then titrated against NaOH solution under nitrogen with a pH meter. The sample densities were measured by using a Paar DMA 602 apparatus incorporating a Hetofrig water bath in order to maintain the measuring cell at constant temperature.

The diffraction experiments were made by using the D4B instrument at the Institut Laue-Langevin, Grenoble. The incident wavelength was 0.7042 Å, and the scattered neutrons were detected with two 64-channel multidetectors, which were calibrated by using the scattering from a vanadium bar. Diffraction patterns were taken for (1) the solutions in their container; (2) the empty solution container; (3) the instrumental background with the sample absent; (4) a cadmium bar of comparable dimensions to that of the sample in order to estimate the background correction at low scattering angles;[16] and (5) a vanadium standard rod of radius 0.4 cm. The solution container was a hollow cylinder of inside radius 0.401 cm and wall thickness 0.029 cm and was fabricated from a titanium–zirconium alloy having a nominal coherent scattering length of zero. The cylinder axis was oriented perpendicular to the incident beam, and the sample temperature was about 23 °C.

The details of the solutions used in the diffraction experiments are given in Table I. The coherent scattering length of the cation in the ^{N}Ni and ^{62}Ni samples was, respectively, 10.3 (1) and −8.2 (2) fm, and the enumerated values of the coefficients A–F in eq 6 and 7 are (mb) 2.71 (3), 7.69 (8), 2.76 (3), 0.072 (8), 0.430 (5), and 0.013 (1), respectively. The scattering length values were taken from ref 17.

Results

The observed total structure factors for the solutions, $^{N}F_0(k)$ and $^{62}F_0(k)$, are shown in Figure 1. Of particular note is the first diffraction peak at 0.54 (2) $Å^{-1}$ in $^{N}F_0(k)$ or 0.52 (2) $Å^{-1}$ in $^{62}F_0(k)$, which is most pronounced for the $^{N}F_0(k)$ sample. The cation isotope dependence of the first diffraction peak shape demonstrates that it has a contribution from the Ni^{2+} correlations, and its position indicates the presence of intermediate range order on a length scale of $11.2 \lesssim r$ (Å) $\lesssim 12.6$.[18] A similar peak is observed in aqueous Ni^{2+} solutions though at higher k values (=0.7–1 $Å^{-1}$).[19,20] By contrast, no such peak is observed for solutions of NaCl in EG.[21]

(14) Squires, G. L. *Introduction to the Theory of Thermal Neutron Scattering*; CUP: Cambridge, 1978.

(15) Cossy, C.; Barnes, A. C.; Enderby, J. E.; Merbach, A. E. *J. Chem. Phys.* **1989**, *90*, 3254.

(16) Bertagnolli, M.; Chieux, P.; Zeidler, M. D. *Mol. Phys.* **1976**, *32*, 759.

(17) Sears, V. F. Thermal Neutron Scattering Lengths and Cross Sections for Condensed Matter Research. Atomic Energy of Canada Ltd. Report AECL-8490, 1984.

(18) Elliott, S. R. *Physics of Amorphous Materials*, 2nd ed.; Longman: Harlow, UK, 1990.

(19) Neilson, G. W.; Howe, R. A.; Enderby, J. E. *Chem. Phys. Lett.* **1975**, *33*, 284.

(20) Neilson, G. W.; Enderby, J. E. *Proc. R. Soc. London* **1983**, *A390*, 353.

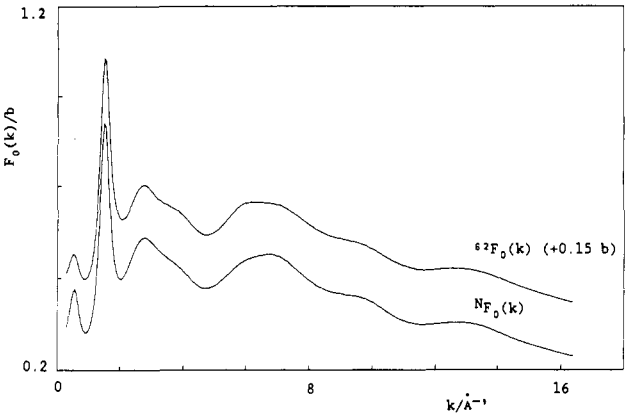

Figure 1. $F_0(k)$ for two different isotopic compositions of nickel in a 0.956 m solution of $Ni(CF_3SO_3)_2$ in deuterated EG.

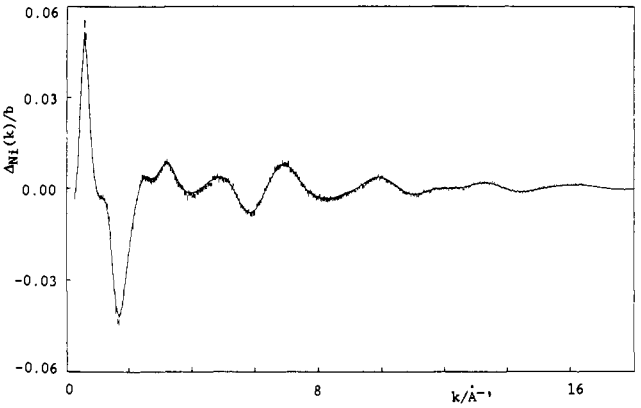

Figure 2. $\Delta_{Ni}(k)$ vs k. The vertical lines show $\Delta_{Ni}(k)$ for a 0.956 m solution of $Ni(CF_3SO_3)_2$ in deuterated EG derived from the $F_0(k)$ of Figure 1. The line size gives the statistical error on the data. The full curve is the solution obtained from a ME analysis of that data and corresponds to the full curve of Figure 3. On the scale of the diagram, the full curve is nearly indistinguishable from that obtained by Fourier back-transforming the $\Delta G_{Ni}(r)$ represented by the points in Figure 3 after setting these points at $\Delta G_{Ni}(0)$ for $r < 1.81$ Å and truncating at 20 Å.

$\Delta_{Ni}(k)$ is illustrated in Figure 2. It was obtained from $\Delta_{Ni}{}^0(k)$ by subtracting a constant of 3.1 mb, which is comparable to the calculated $c_{Ni}[\sigma_{Ni}{}^s - \sigma_{Ni}{}^{si}]/4\pi$ value of 4.7 mb, with *no k-dependent adjustment*. The $\Delta G_{Ni}(r)$ obtained by Fourier transforming $\Delta_{Ni}(k)$ is given in Figure 3. The unphysical features at $r < 1.81$ Å, below the sum of species radii, oscillate about the correct $\Delta G_{Ni}(0)$ value, and there is good agreement between $\Delta_{Ni}(k)$ and the Fourier back-transform of $\Delta G_{Ni}(r)$ obtained after setting $\Delta G_{Ni}(r)$ at $\Delta G_{Ni}(0)$ for $r < 1.81$ Å (see Figure 2). All of these features demonstrate that the $\epsilon'(k)$ term of eq 5 is small, that the cross-sections used in the data analysis are reasonable, and that the measured $\Delta G_{Ni}(r)$ is correctly behaved.

$\Delta G_{Ni}(r)$ was also obtained by a maximum entropy (ME) method (Figure 3) in order to avoid the problems associated with Fourier transforming noisy and truncated k-space data sets:[22] oscillations remain in $\Delta_{Ni}(k)$ at the maximum k value of 16.4 Å^{-1} (see Figure 2). In essence, a smooth real-space $\Delta G_{Ni}(r)$ function is generated in the ME method subject to the constraints that its FT is in agreement with the measured $\Delta_{Ni}(k)$ and that it takes the value $\Delta G_{Ni}(0)$ below the low-r cutoff.[23]

The two $\Delta G_{Ni}(r)$ functions obtained by the ME and FT methods are in good agreement (Figure 3) and reveal three pronounced peaks positioned at 2.04 (2) Å (FT and ME), 2.86 (2) Å (FT),

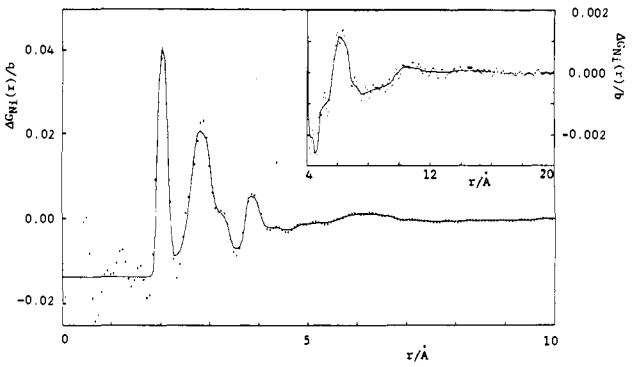

Figure 3. $\Delta G_{Ni}(r)$ vs r. The points give the FT solution for $\Delta G_{Ni}(r)$ obtained from the measured $\Delta_{Ni}(k)$ function of Figure 2 and the full curve gives the ME solution, which corresponds to the full line of Figure 2. The insert gives, on an expanded scale, the details of $\Delta G_{Ni}(r)$ at $r \geq 4$ Å.

or 2.82 (2) Å (ME), and 3.89 (2) Å (FT) or 3.87 (2) Å (ME). The first is readily associated with the Ni^{2+}–O nearest-neighbor correlations on the basis that EG acts as a normal oxygen donor ligand[24] and that, in Ni^{2+} aqueous and methanolic solutions, the average Ni^{2+}–O distance is comparable at 2.07 (2) Å[20,25] or 2.09 (2) Å,[26] respectively. Integration of the first peak over the range $1.81 \leq r$ (Å) ≤ 2.33 to its first minimum gives $\bar{n}_O{}^{Ni} = 5.9$ (1) (FT) or 5.8 (1) (ME), consistent with an octahedral coordination of the Ni^{2+} ion. These $\bar{n}_O{}^{Ni}$ values are comparable to those obtained for concentrated solutions of $NiCl_2$ (4.35 m) and $Ni(ClO_4)_2$ (3.80 m) in D_2O by using the isotopic substitution method in neutron diffraction[20,25] but are significantly greater than the value of 3.7 (2) obtained for a 1 m solution of $NiCl_2$ in methanol.[26] However, in the latter case, there was evidence for inner-sphere complexing of the cation by the anion. An identification of the subsequent peaks in $\Delta G_{Ni}(r)$ requires a detailed consideration of the coordinating nature of the EG ligands.

Discussion

Is the EG Molecule Mono- or Bidentate? Previous work has left it unclear whether EG molecules act as mono- or bidentate ligands on coordinating with the Ni^{2+} ion: there is evidence in the literature for both types of coordinating behavior.[24] The Ni^{2+} complex was therefore simulated by a "ball and stick" approach with a molecular modeling kit. While this kind of simulation is not expected to produce a precise representation of the complex, it will be seen that it does serve to identify the coordinating nature of the EG ligand.

There have been many experimental and theoretical studies of the EG molecular conformations.[7,27-39] Essentially 27 rotational isomers (rotamers) are obtained by allowing each of the torsional

(21) Lond, P. B.; Salmon, P. S. Private communication.
(22) Waser, J.; Schomaker, V. *Rev. Mod. Phys.* **1953**, *25*, 671. Warren, B. E. *X-ray Diffraction*; Addison-Wesley: Reading, MA, 1969; Chapter 10.
(23) Soper, A. K. In *Static and Dynamic Properties of Liquids*, Springer Proceedings in Physics 40; Davidovic, M., Soper, A. K., Eds.; Springer-Verlag: Berlin, 1989. Turner, J.; Soper, A. K.; Finney, J. L. *Mol. Phys.* **1990**, *70*, 679.
(24) Knetsch, D.; Groeneveld, W. L. *Inorg. Chim. Acta* **1973**, *7*, 81; *Recueil* **1973**, *92*, 855.
(25) Newsome, J. R.; Neilson, G. W.; Enderby, J. E.; Sandström, M. *Chem. Phys. Lett.* **1981**, *82*, 399.
(26) Powell, D. H.; Neilson, G. W. *J. Phys.: Condens. Matter* **1990**, *2*, 5867.
(27) Buckley, P.; Giguère, P. A. *Can. J. Phys.* **1967**, *45*, 397.
(28) Matsuura, H.; Miyazawa, T. *Bull. Chem. Soc. Jpn.* **1967**, *40*, 85.
(29) Radom, L.; Lathan, W. A.; Hehre, W. J.; Pople, J. A. *J. Am. Chem. Soc.* **1973**, *95*, 693.
(30) Ha, T.-K.; Frei, H.; Meyer, R.; Günthard, Hs. H. *Theor. Chim. Acta* **1974**, *34*, 277.
(31) Marstokk, K. M.; Møllendal, H. *J. Mol. Struct.* **1974**, *22*, 301.
(32) Almlöf, J.; Siymne, H. *Chem. Phys. Lett.* **1975**, *33*, 118.
(33) Frei, H.; Ha, T.-K.; Meyer, R.; Günthard, Hs. H. *Chem. Phys.* **1977**, *25*, 271.
(34) Walder, E.; Bauder, A.; Günthard, Hs. H. *Chem. Phys.* **1980**, *51*, 223.
(35) Caminati, W.; Corbelli, G. *J. Mol. Spectrosc.* **1981**, *90*, 572.
(36) Takeuchi, H.; Tasumi, M. *Chem. Phys.* **1983**, *77*, 21.
(37) Van Alsenoy, C.; Van Den Enden, L.; Schäfer, L. *J. Mol. Struct.* **1984**, *108*, 121.
(38) Kristiansen, P.-E.; Marstokk, K.-M.; Møllendal, H. *Acta Chem. Scand.* **1987**, *A41*, 403.
(39) Kazerouni, M. R. *Diss. Abstr. Int.* **1988**, *48*, 2336B.

Table II. Assessment of the Models Used to Compare with the $\Delta G_{Ni}(r)$ of Figure 3[a]

designation of model	ϕ_1 (deg)	ϕ_2 (deg)	ϕ_3 (deg)	criterion statisfied? yes (1) or no (0) A	B	C	D	E
MD1 ($\angle$NiO1D1 = 180°)	0	53	−135	1	0	1	1	0
MD2 ($\angle$NiO1D1 = 120°)	0	53	−135	1	1	1	0	0
MLP1	55	54	55	1	0	1	0	0
MLP2	180	59	56	1	1	1	1	0
MLP3	−44	52	62	1	0	1	0	0
MLP4	183	63	183	1	1	1	1	0
MLP5	−48	51	180	1	0	1	0	0
MLP6	−70	49	−70	1	1	1	0	0
MLP7	62	180	62	1	0	0	1	0
MLP8	181	181	64	1	0	0	1	0
MLP9	−53	180	63	1	0	0	1	0
MLP10	180	180	180	1	0	0	1	0
B1 (θ = 0°)	±123 (5)	0	±123 (5)	1	0	0	0	0
B2 (θ = 34 (2)°)	−93 (5) or 150 (5)	0	93 (5) or −150 (5)	1	1	1	1	1
B3	79 (5) or −161 (5)	50 (5)	79 (5) or −161 (5)	1	1	1	1	1

[a] The criteria are described in the text.

(dihedral) angles defined in Figure 4 to take values of 60°, 180°, and −60°. Some of these rotamers are related by rotational symmetry, leaving 10 independent conformations.[7,29,36,37] Of these, the gauche conformations (relative to the C1–C2 bond, i.e., $\phi_2 = \pm 60°$), in which weak intramolecular hydrogen bonds are formed, are the most stable. Recent electron diffraction[39] and microwave spectroscopy[38] results give $\phi_2 \approx 53$–58° for EG in the gas phase. While the previous work does not refer to EG molecules in ionic solution, it provides a starting point for the present simulations. In the latter, the bond lengths were fixed at the values obtained for the gas state (Figure 4a) and the angles $\hat{COD}$, $\hat{CCO}$, and $\hat{CCD}$ were taken to be tetrahedral. Six oxygens were also fixed at the observed distance of 2.04 Å from the Ni^{2+} ion.

The ball and stick models were assessed according to five criteria (A–E) based on the observed $\Delta G_{Ni}(r)$. A successful model was judged to have (A) correlations near to the second peak maximum position ($2.5 \lesssim r$ (Å) $\lesssim 3.2$); (B) correlations on the shoulder at the high-r side of the second peak ($3.2 < r$ (Å) < 3.5); (C) no correlations at the minimum between the second and third peaks ($3.5 \leq r$ (Å) ≤ 3.7); and (D) correlations under the third peak ($3.7 < r$ (Å) < 4.1). Moreover (E) a successful model must give a coordination number for the second peak region that is consistent with the observed area: in addition to the six hydroxyl deuterium atoms associated with the nearest-neighbor oxygens, there is sufficient area under the second peak in $\Delta G_{Ni}(r)$ from $2.3 \lesssim r$ (Å) $\lesssim 3.56$ to account for six carbon atoms and six methyl deuterium atoms. A marking scheme was adopted where a positive answer to any of the criteria scored 1 and a negative answer scored 0 such that a model was judged to be successful only if it scored a total of 5.

In the first step of the analysis procedure, monodentate models were tested wherein the hydroxyl group took a "dipole" configuration with respect to the Ni^{2+} ion;[40] that is, the Ni^{2+} and D1 species were placed in the O1C1C2 plane (models MD1 and MD2). These models were not however consistent with the data (see Table II and Figure 5b). Next, monodentate models were tested wherein the oxygen atoms interact with the Ni^{2+} ion via a lone pair of electrons, giving a tetrahedral $\angle$NiO1C1 angle. All 10 of the rotamers as specified by Podo et al.[7] were used in this analysis (models MLP1 to MLP10), and the lone pair site on the O1 atom was chosen so as to try and maximize the score based on the criteria A–E. It was found that none of the MLP models are fully consistent with the observed $\Delta G_{Ni}(r)$. The basic problem is that each monodentate model gives a coordination number that is too large to be consistent with the measured area under the second peak in $\Delta G_{Ni}(r)$ (criterion E) and few models give correlations around the shoulder on the high-r side of the second peak (criterion B). Attempts made at reducing these problems by

(40) The configurations of water molecules with respect to the Ni^{2+} ion in aqueous solution are discussed by Powell, D. H.; Neilson, G. W. *J. Phys.: Condens. Matter* **1990**, *2*, 3871.

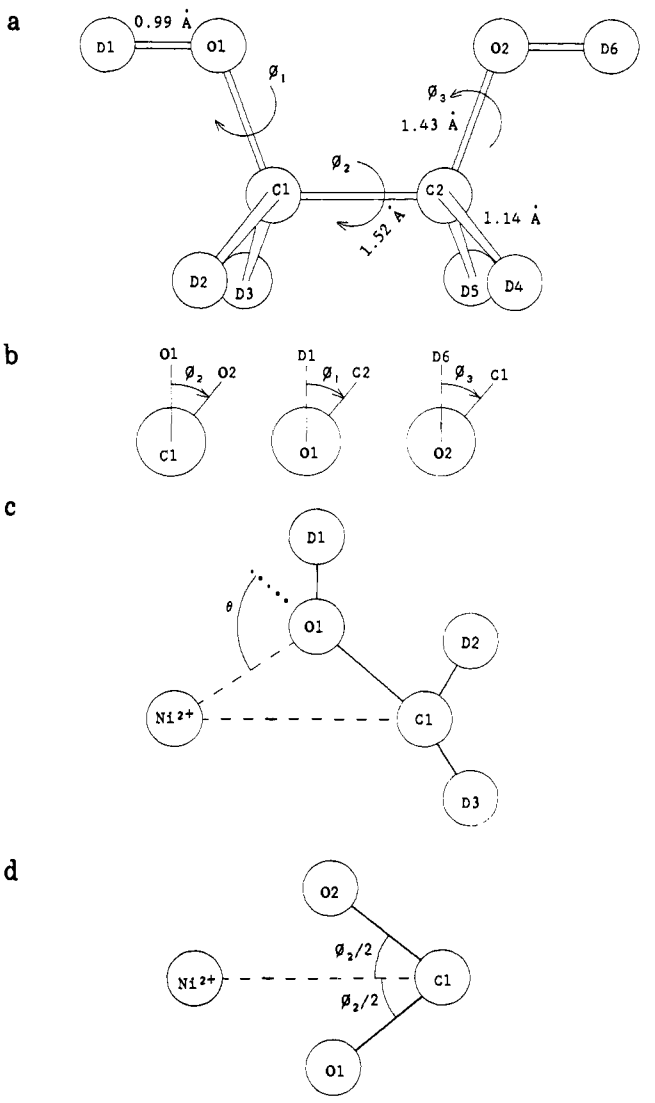

Figure 4. (a) Description of the EG molecule used in modeling the Ni^{2+}–EG complex. ϕ_1, ϕ_2, and ϕ_3 are the torsional angles, and the bond lengths are taken from ref 39. (b) Definition of the positive torsional angles of rotation about the C1–C2, O1–C1, or O2–C2 bonds. A positive sign corresponds to a clockwise rotation of the far group when sighting along the bond. (c) "Angle of tilt" θ between the plane of the EG ligand defined by its two C and two O species and the plane defined by the two O atoms of the EG ligand and the Ni^{2+} ion. The projection is obtained by sighting along the C1–C2 or (equivalently since $\phi_2 = 0$) the O1–O2 bond. (d) Geometry obtained by sighting along the C1–C2 bond for bidentate model B3 wherein $\phi_2 \neq 0$.

Table III. Results Obtained by Fitting $r^2\{\Delta G_{Ni}(r) - \Delta G_{Ni}(0)\}$ to the Sum of Gaussians Represented by Equation 8, Compared to the Distances Obtained from Models B2 and B3[a]

	Gaussian fit			model B2			model B3		
species β	$\bar{n}_\beta^{Ni}$	σ_β (Å)	$r_{Ni\beta}$ (Å)	$r_{Ni\beta}$ (Å)			$r_{Ni\beta}$ (Å)		
O	6.0	0.09	2.05	2.04			2.04		
hydroxyl D	6.0	0.18	2.73	2.54			2.54		
C	6.0	0.15	2.92	2.86			2.86		
methyl D	6.0	0.19	3.31	3.36			3.24		
methyl D	6.0	0.11	3.82	3.82			3.83		
O (2nd shell)	6.0	0.11	4.03	3.92 (X)	4.03 (Y)	4.12 (Z)	3.90 (X)	3.98 (Y)	4.10 (Z)

[a] For the latter a linear hydrogen bond O–D···O of length 1.7 Å (X), 1.8 Å (Y), or 1.9 Å (Z) was assumed. The estimated errors on the distances are ±0.02 Å for the Gaussian fit and ±0.04 Å for models B2 and B3. The estimated errors on the coordination numbers are ±0.2.

changing the torsional angles from those given in Table II did not prove successful; i.e., all of the criteria could not be satisified simultaneously. It was therefore concluded that EG molecules do not act as monodentate ligands on complexing with Ni^{2+} in the present solution.

In the final step of the analysis procedure, several bidentate complexes were modeled where the symmetry was such that the hydroxyl deuteriums, methyl deuteriums, oxygen atoms, and carbon atoms are paired with respect to their radial distances from the Ni^{2+} ion. The NiÔC angles were set at their tetrahedral values; i.e., "lone pair" bonding to the Ni^{2+} ion by the oxygen atoms was assumed. The results are given in Table II and Figure 5b. It was found that a model wherein $\phi_2 = 0$ is consistent with all of the criteria A–E provided that the "angle of tilt" θ (Figure 4c) is finite at ~34 (2)° (cf. models B1 and B2). However, it was also found that all of the criteria were satisfied if (model B3), with θ initially set at zero, a torsional angle $\phi_2 \approx 50°$ is imposed (see Figure 4d). The measured $\Delta G_{Ni}(r)$ is therefore consistent with $Ni(EG)_3^{2+}$ tris-chelate complexes, although a unique conformation cannot be assigned on the basis of the present analysis.

A bidentate coordinating nature for the EG ligand, with respect to the Ni^{2+} ion in solution, is consistent with some of the previous work on Ni^{2+} salts in EG in the crystaline phase.[24] Furthermore it is consistent with the crystal structures observed for Ni^{2+} salts in ethylenediamine ($NH_2CH_2CH_2NH_2$ or en)[41,42] in respect that the Ni^{2+} ion forms a distorted octahedral complex with three en ligands. en is structurally similar to EG, except that the hydroxyl groups are replaced by amine groups. In crystalline $Ni(en_3)(NO_3)_2$, there is a finite torsional angle $\phi_2 \approx 53°$.[41] There is also evidence, from X-ray diffraction, that the en ligand is bidentate in solutions of $Ni(NO_3)_2$ in H_2O/en mixtures.[43]

Interpretation of the Third Peak in $\Delta G_{Ni}(r)$. The third peak of $\Delta G_{Ni}(r)$ is intriguing in that while it readily accommodates at its low-r side the outer-most six deuteriums of the bidentate EG ligands, it has sufficient area to account for many more additional species.

It remains to discuss the possible nature of these species, especially as the third peak is a *pronounced* feature of $\Delta G_{Ni}(r)$: The second solvation shell is usually only observed in neutron diffraction experiments as a broad featureless distribution of correlations.[1]

The solution composition may be expressed as $Ni(CF_3SO_3)_2 \cdot 15.4$ EG. Of the solvent molecules, 3 are inner-sphere-complexed to the Ni^{2+} ion, which leaves 12.4 to be distributed among the anions and second and subsequent coordination shells of the cation. The F or O groups of the triflate anion may account for the additional area under the third peak: as well as the six deuteriums corresponding to the inner-sphere EG ligands, there is sufficient area between $3.56 \lesssim r$ (Å) $\lesssim 4.30$ to accommodate six oxygen or six fluorine atoms. However, unless the triflate anion acts as a tridentate ligand, the solution stoichiometry is such that there is too much area for anions to completely account for the third peak. Furthermore, owing to the 1:6.2 ratio of the anions

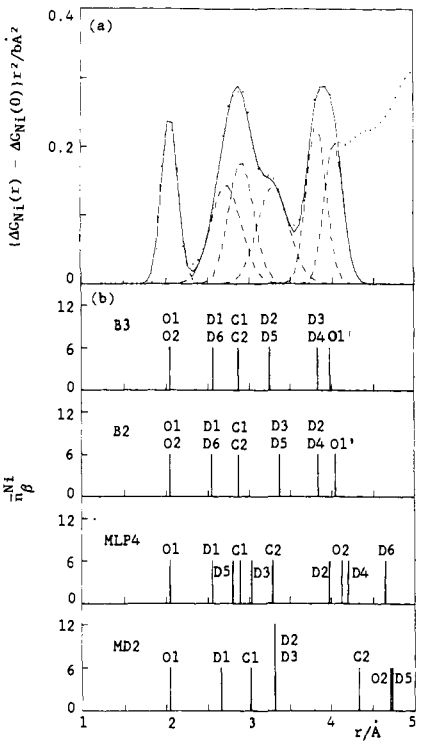

Figure 5. (a) $r^2\{\Delta G_{Ni}(r) - \Delta G_{Ni}(0)\}$ obtained from the ME solution (Figure 3) fitted to six Gaussians represented by the function $f(r)$ of eq 8. The points give the data, the full curve gives the fitted $f(r)$, and the dashed curves give the individual fitted Gaussians. (b) Bar charts representing the mean positions and coordination numbers obtained for selected models of the Ni^{2+}–EG complex (Table II) generated by using a molecular modeling kit (see text). For the bidentate models B2 and B3, the primed species refer to second-shell EG ligands that are bound to the hydroxyl group of the inner-sphere EG ligands via a linear hydrogen bond of length 1.8 Å. For model MD2, the remaining species are located at ~5.20 Å (D4) and ~5.68 Å (D6).

to non-inner-sphere-coordinating EG molecules, it is statistically more likely that the latter have a substantial contribution to the third-peak feature.

There are also strong chemical grounds for attributing the additional third peak area to second-shell solvent ligands since it is possible for such ligands to hydrogen bond to the O–D group of the inner-sphere complex EG molecules without steric hinderance. Indeed, a linear hydrogen bond O–D···O of length 1.7, 1.8, or 1.9 Å between the first and second solvation shell ligands,[8,44] when used in conjunction with either of the successful bidentate models B2 and B3, gives Ni^{2+} to second-shell oxygen correlations *under* the third peak of $\Delta G_{Ni}(r)$ (Figure 5b and Table III).

In view of the molecular nature of the solvent and the apparent success of the ball and stick models in accounting for the main features of $\Delta G_{Ni}(r)$, a profile analysis of the (ME) data was made. This was undertaken by fitting $r^2\{\Delta G_{Ni}(r) - \Delta G_{Ni}(0)\}$ to a sum

(41) Swink, L. N.; Atoji, M. *Acta Crystallogr.* **1960**, *13*, 639. Korp, J. D.; Bernal, I.; Palmer, R. A.; Robinson, J. C. *Acta Crystallogr.* **1980**, *B36*, 560.

(42) Ul-Haque, M.; Caughlan, C. N.; Emerson, K. *Inorg. Chem.* **1970**, *9*, 2421.

(43) Fujita, T.; Ohtaki, H. *Bull. Chem. Soc. Jpn.* **1982**, *55*, 455.

(44) Olovsson, I.; Jönsson, P.-G. In *The Hydrogen Bond*, Schuster, P., Zundel, G., Sandorfy, C., Eds.; North-Holland: Amsterdam, 1976; Vol. 2, Chapter 8.

of Gaussians, representing the individual pair-distribution functions, in the form

$$f(r) = \frac{1}{(2\pi)^{1/2}} \sum_{\beta} A_{\beta} \exp\{-(r - r_{Ni\beta})^2/2\sigma_{\beta}^2\}/\sigma_{\beta} \qquad (8)$$

where A_{β}, $r_{Ni\beta}$, and σ_{β} are, respectively, the area, mean position, and standard deviation of the βth Gaussian. The choice of fitting in $r^2\{\Delta G_{Ni}(r) - \Delta G_{Ni}(0)\}$ space was made since the A_{β} are then directly proportional to the coordination numbers $\bar{n}_{\beta}^{Ni}$. The areas were constrained in the fitting procedure so as to give a 1:1 correspondence between the coordination number of oxygens under the first peak obtained from the first fitted Gaussian and the coordination number obtained from each of the areas of the remaining fitted Gaussians.

The result of fitting six Gaussians to the first three peaks, corresponding to the five Ni^{2+} to first-shell EG ligand species correlations and a further Ni^{2+}–O correlation from a hydrogen-bonded second shell of EG ligands, are given in Figure 5a. The fitted parameters are summarized in Table III where the positions are compared with those obtained from models B2 and B3. The Gaussian fit gives a fair representation of the *profile* of $r^2\{\Delta G_{Ni}(r) - \Delta G_{Ni}(0)\}$, and the fitted peak positions are generally comparable to those obtained from models B2 and B3. This gives credence to a bidentate coordinating nature for EG ligands with respect to the Ni^{2+} ion in solution and shows that the additional area under the third peak can be accounted for by a pair-distribution function that is spatially well defined. A comparison of the fitted Ni^{2+} to second-shell EG oxygen distance with that obtained from models B2 and B3 shows that the data are compatible with the formation of a linear hydrogen bond of length $\sim$1.8 (1) Å between the first and second solvation shell ligands. A coordination number of six EG oxygen atoms in the second shell is consistent with the number of hydroxyl groups available for hydrogen bonding on the inner-sphere EG ligands.

Intermediate Range Order. The $\Delta G_{Ni}(r)$ functions obtained from both the ME and FT solutions show intermediate range order in the range $4.3 \lesssim r$ (Å) $\lesssim 16$ comprising a shoulder at $\sim$5.2 Å, a peak at $\sim$6.09 Å, and a broad feature extending from $10 \lesssim r$ (Å) $\lesssim 16$ (see Figure 3). The latter is consistent with the existence of a first diffraction peak at $\sim$0.56 (2) $Å^{-1}$ in $\Delta_{Ni}(k)$ (Figure 2) and appears to be real in that if $\Delta G_{Ni}(r)$ is truncated at 10 Å and its high r values are set to zero prior to Fourier back-transformation there are small but systematic discrepancies between the back-transform and measured $\Delta_{Ni}(k)$ at low k values. No such discrepancies are observed if $\Delta G_{Ni}(r)$ is truncated at 20 Å as is the case in Figure 2. The nature of the intermediate range order cannot be distinguished on the basis of the present data. However, it is interesting to note that, in liquid glycerol, weak but definite intermolecular order extends to about 20 Å.[8]

Stability of the $Ni(EG)_3^{2+}$ Complex. Although many Ni^{2+}–EG ligand correlations contribute to $\Delta G_{Ni}(r)$, its well-defined profile and in particular the approach of $\Delta G_{Ni}(r)$ to its minimum value of $\Delta G_{Ni}(0)$ after the first peak, supports the assignment of a chelate effect to the Ni^{2+}–EG complex.[45] For such a complex, the Ni^{2+}–EG binding time is expected to greatly exceed the value given by a diffusion-controlled reaction. This latter value can be estimated by using the present data since an EG ligand must diffuse over a distance $\sim$4 Å if it is to leave the $Ni(EG)_3^{2+}$ complex (Figure 3). Incoherent quasi-elastic neutron scattering experiments[46] made by us have given a rough estimate for the average translational proton diffusion coefficient in a 1.16 *m* solution of $Ni(CF_3SO_3)_2$ in EG as 0.05×10^{-9} m^2 s^{-1} at 25 °C. Then by using these estimated values and the expression that the mean square displacement is related to the translational diffusion coefficient D and time t through $\langle r^2 \rangle = 6Dt$, a binding time $\gtrsim 5 \times 10^{-10}$ s is obtained. As might be expected, this value is much less than the actual Ni^{2+}–EG ligand binding time that is given, for EG protons, as 2.3×10^{-4} s at 27 °C.[47]

Conclusion

The main points of the present work are summarized as follows.

(a) EG molecules act as bidentate ligands when coordinating to Ni^{2+} in ethylene glycol solution and give rise to $Ni(EG)_3^{2+}$ tris-chelate complexes.

(b) There is no evidence of substantial inner-sphere complexing by the triflate anion, which supports its use as a noncoordinating species.[3]

(c) The data are consistent with a well-defined hydrogen bond of length $\sim$1.8 (1) Å between the hydroxyl group of the inner-sphere complex EG ligands and the oxygen of the hydroxyl group on second-shell EG molecules. The number of EG oxygen atoms in the second shell that participate in this hydrogen-bonding process is estimated at six.

(d) There is evidence for weak ordering on a length scale of $10 \lesssim r$ (Å) $\lesssim 16$ associated with the Ni^{2+} correlations, as attested to by the low-k position of the first diffraction peak in $\Delta_{Ni}(k)$ and the occurrence of a small feature in $\Delta G_{Ni}(r)$ within this r-space region.

The results demonstrate the wealth of structural information that can be obtained by applying the method of isotopic substitution in neutron diffraction to ions in solution, even when there is a *large* number of near-neighbor ion–solvent molecule correlations. In particular, they show that the $Ni(EG)_3^{2+}$ complex is intimately connected to its surrounding solvent medium.

Acknowledgment. We thank Pierre Chieux for assistance with the diffraction experiment, Phil Gullidge for advice on sample preparation, Roderick Cannon for helpful discussions, Hugh Powell for providing the basis for the Gaussian fitting routine, and the UK SERC for financial support. One of us (P.B.L.) thanks the SERC for a studentship during the tenure of which this work was carried out. He thanks the staff of Billings and the GSA and Chris Benmore and Ian Penfold whose good-humored support has been invaluable.

(45) Cotton, F. A.; Wilkinson, G. *Advanced Inorganic Chemistry*, 5th ed.; Wiley: New York, 1988; p 45.
(46) Salmon, P. S. *J. Phys. C: Solid State Phys.* **1987**, *20*, 1573. Herdman, G. J.; Salmon, P. S. *J. Am. Chem. Soc.* **1991**, *113*, 2930.
(47) Pearson, R. G.; Lanier, R. D. *J. Am. Chem. Soc.* **1964**, *86*, 765.